Isospin decomposition of the Gamow-Teller strength in Cu-58

Fujita, Y; Akimune, H; Daito, I; Fujiwara, M; Harakeh, M N; Inomata, T; Janecke, J; Katori, K; Nakada, H; Nakayama, S

Published in:
Physics Letters B

DOI:
10.1016/0370-2693(95)01304-0

Publication date:
1996

4 January 1996

PHYSICS LETTERS B

ELSEVIER

Physics Letters B 365 (1996) 29–34

Isospin decomposition of the Gamow–Teller strength in ^{58}Cu

Y. Fujita [a], H. Akimune [b], I. Daito [b], M. Fujiwara [b], M.N. Harakeh [c], T. Inomata [a], J. Jänecke [d], K. Katori [a], H. Nakada [e], S. Nakayama [f], A. Tamii [g], M. Tanaka [h], H. Toyokawa [b], M. Yosoi [g]

[a] *Department of Physics, Osaka University, Toyonaka, Osaka 560, Japan*
[b] *RCNP, Osaka University, Ibaraki, Osaka 567, Japan*
[c] *KVI, Zernikelaan 25, 9747 AA Groningen, The Netherlands*
[d] *Department of Physics, University of Michigan, Ann Arbor, MI 48109-1120, USA*
[e] *Department of Physics, Chiba University, Inage, Chiba 263, Japan*
[f] *Department of Physics, Tokushima University, Tokushima 770, Japan*
[g] *Department of Physics, Kyoto University, Sakyo, Kyoto 606, Japan*
[h] *Kobe Tokiwa Jr. College, Nagata, Kobe 653, Japan*

Received 13 September 1995
Editor: R.H. Siemssen

Abstract

The Gamow–Teller (GT) strength excited by a (p, n)-type reaction on a nucleus with isospin T_0 and $N > Z$ is shared by isospin components $T_0 - 1$, T_0 and $T_0 + 1$. A good energy resolution (^{3}He, t) reaction on ^{58}Ni revealed the fine structure of the GT strength in ^{58}Cu. The isospin of each level constituting the fine structure was assigned by comparing to results from inelastic electron and proton scatterings and (n, p)-type reactions, thus resolving the isospin structure of the GT strength in ^{58}Cu. The ratio of the summed GT strengths among the three isospin components is well described by a shell-model calculation.

PACS: 25.55.Kr; 24.30.Cz; 27.40. + z

Keywords: ^{58}Ni target; (^{3}He, t); Good resolution; Gamow–Teller strength; Fine structure; Isospin; Isospin structure

The $J^\pi = 1^+$ Gamow–Teller (GT) state is characterized as an $L = 0$ spin–isospin excitation. It has been clearly observed at 0° in various charge-exchange reactions and at bombarding energies exceeding 100 MeV/u, where the nuclear interaction favors the spin–isospin excitations. In a (p, n)-type reaction on a target nucleus having an isospin value $T = T_0$ larger than one, where T_0 is defined by $T_0 = (N - Z)/2$, the GT strength in the daughter nucleus is distributed over states with final isospin values $T = T_0 - 1$, T_0 and $T_0 + 1$. The three T components split by the symmetry energy, where the lowest, intermediate and highest T components are located at the lowest, intermediate and highest excitation energies, respectively.

In first-order approximation, the transition strength to each T component is proportional to the square of the Clebsch–Gordan (CG) coefficient of isospin cou-

SSDI 0370-2693(95)01304-0

pling. For a heavy nucleus with large T_0, the CG coefficient for the transition to the $T_0 - 1$ component is much larger than the others. Most of the GT strength, therefore, is exhausted by the $T_0 - 1$ component forming a bump-like structure commonly denoted as the Gamow–Teller resonance (GTR). Since the time of the pioneering (p, n) experiments on ^{90}Zr and ^{208}Pb targets at $E_p = 200$ MeV [1,2] and (^{3}He, t) experiments at intermediate energies [3], the GT strength has been perceived as a single broad peak (GTR) with often a few associated low-lying discrete states as reviewed in Ref. [4].

The situation is different for a target nucleus with a small T_0. ^{58}Ni has a ground-state isospin $T_0 = 1$, and the square of the CG coefficient of isospin coupling leads to a transition strength ratio of 2 : 3 : 1 for the $T_0 - 1$, T_0 and $T_0 + 1$ components, respectively. The $J^\pi = 1^+$ GT strength excited in ^{58}Cu, therefore, is expected to spread more or less evenly over the three isospin components.

Inelastic scattering reactions, like (p, p′) or (e, e′), can populate $L = 0$, spin-excitation states called M1 states. Taking the Wigner supermultiplet scheme, the M1 states are the analog states of either the T_0 or $T_0 + 1$ GT states. The transition strength ratio, however, is different from that in the (p, n)-type reaction; for the $T_0 = 1$ target nucleus ^{58}Ni, it is 1 : 1 for the T_0 and $T_0 + 1$ components again from the square of the CG coefficient. Furthermore, the (n, p)-type charge-exchange reactions only populate GT states that are analogs to the $T_0 + 1$ part of the GT states populated in the (p, n)-type reactions.

Basically the comparison among the different probes can identify the isospin structure of the GT strength [5], but practically it was not easy to achieve this mainly due to the limited energy resolution attainable in the (p, n)-type reactions at an incident energy higher than 100 MeV/u. This letter reports on the identification of the isospin structure of the GT strength in ^{58}Cu through comparing the fine structure observed in a good resolution ^{58}Ni(^{3}He, t) experiment performed at 0° to the structure observed in inelastic electron and proton scatterings as well as in (n, p)-type reactions on a ^{58}Ni target.

The experiment was performed by combining the 150 MeV/u ^{3}He beam from the $K = 400$ RCNP ring cyclotron [6] with the QQDD-type spectrometer Grand Raiden [7]. A 5.8 mg/cm^2 ^{58}Ni foil with an enrichment of 99.9% was bombarded by about 5 nA ^{3}He^{2+} beam. In order to improve the energy resolution, the dispersion-matching technique was used for beam transportation. The spectrometer was set at 0° and scattered particles were accepted within ± 20 mr in both horizontal (x) and vertical (y) directions. The magnetic field was adjusted to select outgoing tritons. The ^{3}He^{2+} beam, due to its small bending radius, was stopped by a Faraday cup placed inside the first dipole magnet. After momentum analysis by the spectrometer, tritons were detected with a ray-trace-type multi-wire drift-chamber system [8]. More details of the experiment can be found in Ref. [9].

The raytrace information made it possible to subdivide the acceptance angle of the spectrometer by a software cut. Fig. 1(a) shows the 0° spectrum for the angular range ± 5 mr in the x direction (no cut is made in the y direction). With an achieved energy resolution of 140 keV, the fine structure of the main GT strength at around $E_x = 9$ MeV, which was observed more or less as a single broad bump in (p, n)-type reactions, was revealed. In addition, several sharp peaks are observed up to $E_x = 13$ MeV. The gross feature of the spectrum, however, is quite similar to that observed in the ^{58}Ni(p, n) reaction at $E_p = 120$ and 160 MeV [10]. This fact agrees with the report that the (^{3}He, t) reaction at a bombarding energy exceeding 100 MeV/u is a single-step direct reaction, and that the relevant effective interactions $V_{\sigma\tau}$ and V_τ, are similar in both (p, n) and (^{3}He, t) reactions at a similar incident energy per nucleon [3,11,12]. The present (^{3}He, t) reaction at 150 MeV/u with a better energy resolution is, therefore, suited for the detailed investigation of the GT strength.

Not much is known about the excitation energies of 0^+ and 1^+ states in ^{58}Cu [13]. The excitation energy of the main GTR region was calibrated in the present experiment via the calculation of kinematics using well-known low-lying discrete states observed in the ^{12}C and ^{13}C(^{3}He, t) spectra as references. These spectra were measured and analyzed under the same conditions as those for the ^{58}Ni run. Owing to the large Q-value of the ^{12}C(^{3}He, t) reaction, the excitation energy of ^{58}Cu was determined up to 13 MeV by interpolation. In this region, we estimate that the uncertainties in excitation energies are less than 50 keV. The excitation energies are in fairly

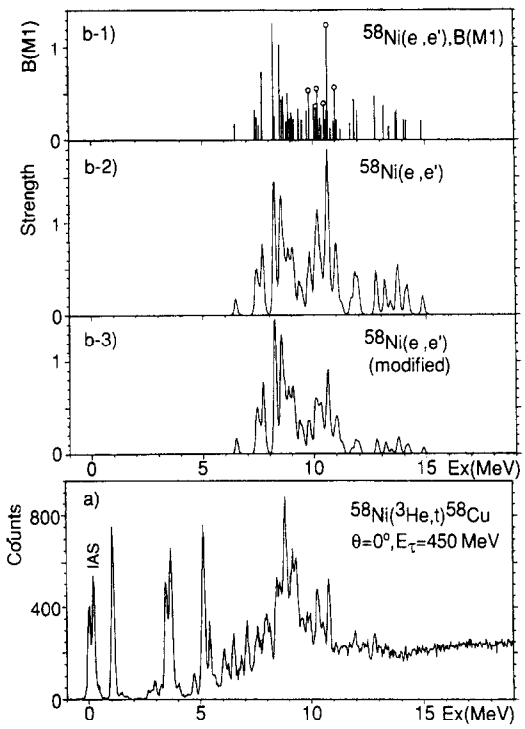

Fig. 1. Comparison between the 0° ^{58}Ni(^{3}He, t) spectrum and the M1 strength distribution obtained in the ^{58}Ni(e, e′) experiment [15]. (a) The 0° ^{58}Ni(^{3}He, t) spectrum; for details, see text. (b-1) The B(M1) distribution obtained in the ^{58}Ni(e, e′) experiment. (b-2) The reconstructed (e, e′) spectrum after convoluting with the experimental energy resolution of the (^{3}He, t) experiment. (b-3) The same as (b-2), but T_0+1 strength being reduced artificially by a factor of three. Figure (b) is shifted with an excitation energy of 0.20 MeV relative to figure (a), since the isobaric analog state (IAS) of ^{58}Ni, 0^+ ground state is observed at $E_x = 0.20$ MeV in ^{58}Cu.

good agreement with those of the (p, n) measurements [10].

Among the T_0-1, T_0 and T_0+1 components of the GT strength, the T_0-1 part is identified through the non-existence of the corresponding M1 strength in the inelastic scattering experiments, and T_0 and T_0+1 parts through their existence. For such a comparison, the M1 strength distributions deduced from (p, p′) at $E_p = 200$ MeV [14] and from (e, e′) [15] are valuable. Especially in the latter, the B(M1) strength was mapped with a resolution of 30 keV in the excitation energy range $E_x = 5.9$–15.0 MeV. The B(M1) distribution is shown in Fig. 1(b-1). The two humps at the center-of-gravity energies $E_x = 8.4$ and 11.4 MeV were tentatively identified respectively as T_0 and T_0+1 components of the M1 excitation from energy systematics [15].

The T_0+1 component was studied with the ^{58}Ni(t, ^{3}He)^{58}Co reaction at $E_t = 25$ MeV [16]. In the low-lying region, $E_x = 1.05$–2.25 MeV in ^{58}Co, six 1^+ GT states were identified via their angular distributions. Again assuming the Wigner supermultiplet scheme, the analog state to the first T_0+1, 1^+ state is expected at $E_x = 9.82$ MeV in an inelastic scattering experiment. In fact corresponding states have been identified in the $E_x = 9.85$–11.01 MeV region of the (e, e′) spectra for all of the six states [15]. The six states marked with the small circles on top of the vertical lines in Fig. 1(b-1) are the main strengths in the second hump. Further information on the T_0+1 component was obtained by a recent ^{58}Ni(n, p)^{58}Co reaction at $E_n = 198$ MeV [17]. Due to insufficient energy resolution, no discrete level was resolved, but it was found that T_0+1 GT strength continuously existed from $E_x = 1$ MeV up to 5 MeV. In order to account for the T_0+1 GT strength, it is natural to assume that the 1^+ states observed at $E_x > 11.5$ MeV in the (e, e′) spectra are of T_0+1 nature.

In order to make the (e, e′) results more comparable with the (^{3}He, t) spectrum, the B(M1) distribution (Fig. 1(b-1)) was convoluted with the peak shape of the well-separated $E_x = 1.05$ MeV level in the (^{3}He, t) spectrum. The reconstructed (e, e′) spectrum shown in Fig. 1(b-2) looks rather different from the (^{3}He, t) spectrum of Fig. 1(a). (For the 0.20 MeV offset in excitation energy, see the caption of Fig. 1.) It should, however, be noted that for the direct comparison the difference in strength due to the CO coefficients of the isospin coupling should be taken into account. For the $T_0 = 1$ target ^{58}Ni, the T_0+1 strength is a factor of three smaller in the (^{3}He, t) reaction than in the (e, e′) reaction. The modified (e, e′) spectrum in which the strengths of all T_0+1 candidates are reduced by the factor of three is shown in Fig. 1(b-3). This spectrum looks now very similar to the (^{3}He, t) spectrum considering that the B(M1) strength excited in the (e, e′) reaction includes not only the spin contribution but also the orbital contribution, which can make the spectrum look somewhat different. It can noted that to each peak structure in the modified (e, e′) spec-

trum, a corresponding peak is observed in the (^{3}He, t) spectrum up to nearly $E_x = 14$ MeV.

The present (^{3}He, t) spectrum was decomposed into levels by taking the shape of the 1.05 MeV level as a response function. Since sharp peaks were observed even in the high excitation region, decomposition was performed by using the same response function up to $E_x = 15$ MeV, and by assuming enough number of levels so as to reproduce all the observed counts of the spectrum.

The isospin of each level was assigned by examining whether or not the corresponding part could be found in the modified (e, e′) spectrum. Below $E_x =$ 10 MeV, the isospin $T = T_0 - 1$ was assigned to all the levels not observed in the (e, e′) spectrum. A few exceptions are the 0.20 MeV level, which is the isobaric analog state (IAS) of ^{58}Ni, 0^+ ground state (g.s.) and the 5.43 MeV level, which corresponds to the 1^+ state observed in (p, p′) reactions at $E_x = 5.17$ MeV [18,19], thus suggesting a $T = T_0$ assignment. To the levels above 11.7 MeV and having a counterpart in the reconstructed (e, e′) spectrum, an isospin $T_0 + 1$ was assigned.

As inferred by the (e, e′) and (t, ^{3}He) results, T_0 and $T_0 + 1$ strengths are mixed in the region $E_x =$ 10–11.7 MeV, and they form together several peaks in the (^{3}He, t) spectrum (see Fig. 1(a)). The assignment of the isospin was not so easy on a level-by-level base. Instead, we used a practical way to estimate the strengths for the two components. The count sum for each peak was distributed to T_0 and $T_0 + 1$ components by the ratio of T_0 and $T_0 + 1$ B(M1) strengths of the corresponding peak in the modified (e, e′) spectrum.

How to subtract "background" is still a current issue in the region of higher excitation. Since the neutron separation energy is high (Sn = 12.4 MeV) in ^{58}Cu, almost no contribution is expected from the neutron decay. The proton-decay channel opens at $E_x = 2.9$ MeV, but the observation of narrow peaks up to $E_x = 13$ MeV suggests that the contributions from the sequential proton decay as well as from the direct proton decay (quasi-free scattering) are not so large [20,21]. In the present analysis, no background was subtracted following the analysis of the ^{58}Ni(p, n) work [10]. It is also known that the 0° spectra contain backgrounds due to $L = 1$ and 2 excitations. The (p, n) work showed through the angular distribution analysis that the ratio of the $L = 0$ cross section to the total was almost unity below $E_x = 10$ MeV, but decreased at higher E_x; at 0° the reported ratios were about 0.84 and 0.53 for the energy intervals $E_x = 10$–12 and 12–14 MeV, respectively. In the present analysis, the ratios of counts of the GT strength to the total counts are 0.85 and 0.45 for these intervals, respectively.

For the (p, n) reaction at bombarding energies exceeding 100 MeV, it has been demonstrated that the 0° cross section is proportional to the B(GT) value [22,23], and the same is suggested for the (^{3}He, t) reaction at 150 MeV/u [11,12,24]. The GT strength for the ^{58}Ni(^{3}He, t)^{58}Cu(g.s.), i.e. $0^+ \rightarrow 1^+$ transition, is deduced to be $B(\mathrm{GT}) = 0.163 \pm 0.004$ from the experimentally known ft-value $\log ft = 4.86 \pm 0.01$ for the allowed β-decay from ^{58}Cu(g.s.) to ^{58}Ni(g.s.) [25]. Since the 1^+ g.s. and the 0^+ IAS at $E_x = 0.20$ MeV were resolved in the present measurement, a reliable peak count was obtained for the g.s. The relationship between the peak count and the B(GT) value of the g.s. was simply extended to obtain the B(GT) value of each GT level [23].

The obtained B(GT) strengths are given in Table 1. It is noted that more B(GT) strength resides in the $T_0 - 1$ component and less by the T_0 component than expected from the ratio of 2:3 estimated from the square of the CG coefficients. The difference in the ratio is partly understood from a naive shell model picture. Assuming 28 protons and neutrons are filled up to the $f_{7/2}$ shell (^{56}Ni core) and two additional neutrons are filled in the $p_{3/2}$ shell in the g.s. of ^{58}Ni, the 1^+, GT states are formed by the configurations $(\pi p_{3/2}, \nu p_{3/2}^{-1})$, $(\pi p_{1/2}, \nu p_{3/2}^{-1})$ and $(\pi f_{5/2}, \nu f_{7/2}^{-1})$. It is, however, argued from the isospin selection rule that only the $(\pi f_{5/2}, \nu f_{7/2}^{-1})$ configuration can take part in the formation of the $T_0 + 1$ component [26]. Similarly it is argued that two $p_{3/2}$ particles on top of the ^{56}Ni core cannot form a $J^\pi = 1+$, $T = 1$ state due to Pauli principle. Namely only the latter two configurations can contribute to the T_0 component. On the other hand, all three configurations can contribute to the $T_0 - 1$ component. If these effects are properly taken into account, it is calculated that the expected B(GT) strength of 19.7 is shared by the $T_0 - 1$, T_0 and $T_0 + 1$ isospin components with the ratio of 47%, 41% and 12%, respectively.

For the further understanding of the sharing of the B(GT) strength in ^{58}Cu, a large-scale shell-model calculation has been performed assuming ^{40}Ca to be a doubly-magic inert core. The calculation which uses the Kuo–Brown G-matrix interaction and empirical single-particle energies succeeded in describing various properties of nuclei in the middle pf-shell [27]. As listed in Table 1, the strength ratios of the three isospin components are similar to the ones obtained in the naive shell model picture given above. The strength ratio of the T_0 to the $T_0 - 1$ components is 0.85 in the calculation, while the experiment gives 1.1 ± 0.3. The experimental result is reproduced by the calculation; the T_0 component carries less GT strength relative to the $T_0 - 1$ component than expected from the isospin CO coefficients, which yield the ratio of 1.5. The observed $T_0 + 1$ percentage is larger than the shell model prediction. This may indicate that some amount of "background", probably due to the quasi-free charge-exchange scattering, should be subtracted in the energy region where the $T_0 + 1$ states exist [20].

The B(GT) strength distributions experimentally extracted for the three isospin components are shown in Fig. 2. The strengths are convoluted with the peak shape of the 1.05 MeV level in order to make a direct comparison with the raw spectrum shown in Fig. 1(a). We note that the main bump-like structure observed at around $E_x = 9$ MeV consists of the T_0 component. Remember that the GTR observed in a (p, n)-type reaction on a heavier nucleus with a large T_0 value is of $T_0 - 1$ nature.

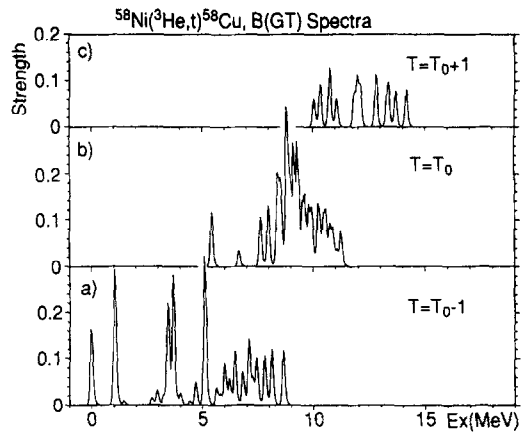

Fig. 2. The B(GT) strength distributions for the three isospin components convoluted with the experimental response function. (a) B(GT) spectrum for the $T = T_0 - 1$ component. (b) B(GT) spectrum for the $T = T_0$ component. (c) B(GT) spectrum for the $T = T_0 + 1$ component.

The $T_0 - 1$ component is widely fragmented, and it looks that the strength is roughly classified into three groups centered at 0.7 MeV, 4 MeV and 7 MeV. As mentioned above, the 1^+, $T_0 - 1$ component can be formed by the shell configurations $(\pi p_{3/2}, \nu p_{3/2}^{-1})$, $(\pi p_{1/2}, \nu p_{3/2}^{-1})$ and $(\pi f_{5/2}, \nu f_{7/2}^{-1})$. It is interesting to point out that the differences of particle–hole energies among these configurations [27] are more or less similar to the differences of the centroid energies of the three groups.

The T_0 component concentrates in the region $E_x = 7.5$–11.5 MeV. One of the exceptions is the 5.43 MeV state. The analog M1 state observed at $E_x = 5.17$ MeV in the $(\vec{p},p')$ study is assigned the $(p_{1/2}, p_{3/2}^{-1})$ configuration from the analysis of the analyzing power [19]. Furthermore, four M1 states were reported in the energy region corresponding to $E_x = 8$–10 MeV in ^{58}Cu. Two of them are identified to be mainly of $(p_{1/2}, p_{3/2}^{-1})$ configuration and the other two to be of $(f_{5/2}, f_{7/2}^{-1})$ configuration. Thus it is inferred that the states with two different configurations are mixed in the main peak.

The expected main configuration of the $T_0 + 1$

Table 1
Absolute and relative B(GT) strengths for the three isospin components in ^{58}Cu and the total B(GT)

	$T_0 - 1\,(=0)$	$T_0\,(=1)$	$T_0 + 1\,(=2)$	Total
(p, n) [a]				7.8 ± 1.9
(^{3}He, t) [b]	2.5 ± 0.3	2.8 ± 0.5	1.0 ± 0.4	6.3 ± 0.6
(^{3}He, t) [c]	40%	44%	16%	
Isospin CG [d]	33%	50%	17%	
Shell model [e]	49%	41%	10%	

[a] Ref. [10].
[b] Present experiment.
[c] Ratios of B(GT) strengths from the present experiment in percentage.
[d] Ratios of B(GT) strengths expected on basis of the square of isospin CG coefficients in percentage.
[e] Ratios of B(GT) strengths predicted by a large-scale shell-model calculation in percentage.

component is $(\pi f_{5/2}, \nu f_{7/2}^{-1})$ In fact, the analog M1 state for the 10.80 MeV peak is identified to have the configuration $(f_{5/2}, f_{7/2}^{-1})$ in the $(\vec{p},p')$ study [19].

Finally, the total B(GT) strength given in Table 1 is in reasonable agreement with that of the (p, n) result [10]. The strength, however, is only one third of that expected on basis of the naive shell model (i.e., 19.7). The reduction in B(GT) strength can be understood to result from RPA-type correlations peculiar to fp-shell nuclei [28], and from a universal quenching factor of 0.6 as deduced from the systematics for heavy-mass nuclei [5].

In summary, with a good energy-resolution study of the GT strength in ^{58}Cu using the (^{3}He, t) reaction, it is indicated that the usual broad bump of the GTR resolves into fine structure. By comparing the present good resolution ^{58}Ni(^{3}He, t) spectrum with the results from (e, e'), (p, p'), (t, ^{3}He) and (n, p) reactions, one of the isospin values $T_0 - 1$, T_0 and $T_0 + 1$ was assigned to each level constituting the fine structure. The ratio of the summed B(GT) strengths for the $T_0 - 1$ and T_0 components is well explained by the result of the large-scale shell-model calculation. The B(GT) strength distribution was reconstructed for each isospin component. The $T_0 - 1$ component is widely fragmented, while the T_0 component is rather concentrated at around $E_x = 9$ MeV.

The authors are grateful to the crew of RCNP ring cyclotron for their efforts in providing a good quality ^{3}He beam. The present work was performed under the auspices of the U.S.–Japan cooperative science program by JSPS and NSF. The experiment was performed at RCNP, Osaka under the experimental program number E54.

References

[1] D.E. Bainum et al., Phys. Rev. Lett. 44 (1980) 1751.
[2] D.J. Horen et al., Phys. Lett. B 95 (1980) 27.
[3] C. Ellegaard et al., Phys. Rev. Lett. 50 (1983) 1745.
[4] F. Osterfeld, Rev. Mod. Phys. 64 (1992) 491.
[5] C. Gaarde, Nucl. Phys. A 396 (1983) 127c.
[6] I. Miura et al., RCNP annual report (Osaka Univ., 1991) p. 149.
[7] M. Fujiwara et al., RCNP annual report (Osaka Univ., 1991) p. 173.
[8] T. Noro et al., RCNP annual report (Osaka Univ., 1991) p. 177.
[9] H. Akimune et al., Phys. Rev. C 52 (1995) (in print).
[10] J. Rapaport et al., Nucl. Phys. A 410 (1983) 371.
[11] I. Bergqvist et al., Nucl. Phys. A 469 (1987) 648.
[12] H. Akimune et al., Nucl. Phys. A 569 (1994) 245c; M. Fujiwara et al., Nucl. Phys. A 577 (1994) 43c.
[13] L.K. Peker, Nucl. Data Sheets 61 (1990) 189.
[14] C. Djalali et al., Nucl. Phys. A 388 (1982) 1; N. Marty et al., Nucl. Phys. A 396 (1983) 145c.
[15] W. Mettner et al., Nucl. Phys. A 473 (1987) 160.
[16] F. Ajzenberg-Selove et al., Phys. Rev. C 30 (1984) 1850; F. Ajzenberg-Selove et al., Phys. Rev. C 31 (1985) 777.
[17] S. El-Kateb et al., Phys. Rev. C 49 (1994) 3128.
[18] M. Fujiwara et al., Nucl. Phys. A 410 (1983) 137.
[19] K. Hosono et al., Nucl. Phys. A 454 (1986) 237.
[20] F. Osterfeld, Phys. Rev. C 26 (1982) 762.
[21] E. Caurier, A. Poves and A.P. Zuker, Phys. Rev. Lett. 74 (1995) 1517.
[22] C.D. Goodman et al., Phys. Rev. Lett. 44 (1980) 1755.
[23] T.N. Taddeucci et al., Nucl. Phys. A 469 (1987) 125.
[24] A. Brockstedt et al., Nucl. Phys. A 530 (1991) 571.
[25] H.W. Jongsma et al., Nucl. Phys. A 179 (1972) 554.
[26] A. Bohr and B.R. Mottelson, Nuclear Structure, Vol. 1 (Benjamin, New York, 1969).
[27] H. Nakada, T. Sebe and T. Otsuka, Nucl. Phys. A 571 (1994) 467.
[28] N. Auerbach et al., Nucl. Phys. A 556 (1993) 190.